

## AuGeNi OHMIC CONTACTS TO *n*-InP FOR FET APPLICATIONS

JESÚS A. DEL ALAMO† and TAKASHI MIZUTANI

NTT LSI Laboratories, 3-1 Morinosato Wakamiya, Atsugi, 243-01 Japan

(Received 26 May 1988; in revised form 29 June 1988)

**Abstract**—AuGeNi ohmic contact formation on Si-implanted InP has been investigated. Ohmic contacts suitable for application to field-effect transistors are obtained at alloying temperatures between 360°C and 630°C, with contact resistance around 0.02–0.07 Ω·mm. A liquid phase appears at an alloying temperature of about 460°C. In consequence, contacts with excellent surface morphology and edge definition are obtained for alloying temperatures between 360°C and 460°C. Four different regimes in the alloying temperature behavior of the AuGeNi/InP system are observed and their physical origin is discussed. A close to quadratic correlation exists between the achieved contact resistance and the underlying semiconductor sheet resistance.

### INTRODUCTION

The fabrication of field-effect transistors (FETs) using InP as active material is being pursued with intensity[1,2] due to the higher peak velocity of electrons[3] and smaller ionization coefficients[4] of InP, as compared with GaAs. These characteristics make InP FETs suitable candidates for high-power microwave amplification. In addition, semiconductors lattice matched to InP constitute the stepping stone of optical devices for long-wavelength optical-fiber communications. FETs fabricated on InP substrates are being explored in pursuit of optoelectronic integrated circuits[5].

To exploit these intrinsic advantages of InP, the influence of the extrinsic elements of the FET has to be minimized. An important one is the contact resistance between the semiconductor source and drain regions and the interconnect metallization. For the contact resistance,  $R_c$ , not to degrade the intrinsic transconductance,  $g_{mo}$ , of an FET, its value has to be  $R_c < 1/g_{mo}$ . This condition requires values of  $R_c$  smaller than 0.1 Ω·mm. To our knowledge, the only metallization system that has achieved values of this order on *n*-InP is the AuGeNi alloyed contact scheme[6].

In spite of the excellent performance of AuGeNi ohmic contacts to InP, ohmic contact formation as a function of alloying temperature in this widely used metallization system has received little attention. Additionally, the many demands imposed on a practical metallization scheme from the point of view of process compatibility, surface morphology, and edge definition, have not been properly addressed, if at all, in the case of AuGeNi/*n*-InP. This paper intends to fill this gap by studying the process of ohmic contact

formation and degradation as a function of alloying temperature of the AuGeNi system alloyed on InP. A wide alloying temperature window optimum for FET application is found with contact resistance in the required range.

### EXPERIMENTAL

The starting material was polished semi-insulating Fe-doped (100) InP substrates. Prior to processing, the surface was etched using the technique of Nishitani and Kotani[7]. Si ion implantation was carried out at 100 keV to a dose of  $5 \times 10^{13} \text{ cm}^{-2}$ . The implanted ions were activated by lamp annealing at 750°C during 4 s using a GaAs proximity cap[8]. The resulting layer sheet resistance was about 200–350 Ω/□. Calculations using LSS statistics and accounting for the partial activation of the implanted species predict a peak doping level of about  $8 \times 10^{17} \text{ cm}^{-3}$ . Subsequently, mesa isolation was carried out by chemical etching. The ohmic metal consisted of 1500 Å of AuGe (Ge 12% by weight) followed by 300 Å of Ni evaporated in an electron-beam system. The base pressure before evaporation was in the low  $10^{-7}$  torr range. Ohmic pattern definition was performed by lift-off.

The sample was then divided in small pieces and each one alloyed at a different temperature using an infrared lamp. The alloying ambient was N<sub>2</sub> at atmospheric pressure. The alloying cycle consisted of a 100°C/min ramp-up, followed by a 30 s holding time at the alloying temperature, and a free ramp-down. The alloying temperature is known within  $\pm 4^\circ\text{C}$ . At this point in the process a number of measurements, described below, were taken. Subsequently, on a few specimens, overlayers of Ti (300 Å) and Au (2000 Å) were evaporated and patterned by lift-off. Contact resistance measurements were again carried out. In a

†Present address: Massachusetts Institute of Technology, Room 13-3062, Cambridge, MA 02139, U.S.A.

few cases, the Si implantation conditions (energy and/or dose) and the implant annealing temperature were changed in order to produce  $n^+$  layers of different sheet resistance.

Transmission Line Method (TLM) measurements[9] were carried out using the four-point probe technique. The ohmic pads were separated 2, 3, 5, 10, 20 and 30  $\mu\text{m}$ . The metal pads were 115  $\mu\text{m}$  long and 100  $\mu\text{m}$  wide. The linearity of the  $I$ - $V$  characteristics was verified in all cases. The contact resistance was extracted by extrapolating the measured TLM resistance to zero spacing using a least-squares technique (in all low-resistance contacts, the regression coefficient of the fit was better than 0.9999). From this intercept resistance, the contact resistance per unit length ( $R_c$ ), also denoted as specific transfer resistance, is immediately extracted[9]. This is the proper figure of merit for lateral devices, like FETs.

The ohmic pad sheet resistance,  $R_m$  (alloyed metal-semiconductor layer structure), was measured by means of a  $20 \times 1000 \mu\text{m}^2$  pattern also using the four-point probe technique. As shown later, this parameter provided important information on the metallurgical reactions occurring during the alloying process.

The surface morphology of the contact pad is an additional important consideration in the manufacture of complex circuits. Surface roughness reduces device yield, especially when multilevel interconnects and air bridges are used. Therefore, in this work, the contact surface roughness was monitored by means of a Tencor Alpha-Step 200. A good edge definition of the contact pad is also essential for advanced FET structures in which the gate-source distance has to be made as small as possible. The edge of the ohmic contacts was investigated by scanning electron microscopy. Finally, sputter auger profiles of all the atomic elements involved in the metallization were taken in selected samples.

## RESULTS

Figure 1 shows the measured contact resistance as a function of alloying temperature for as-alloyed samples and Ti/Au-covered samples. The contacts become ohmic at around 300°C. A broad minimum in  $R_c$  is obtained from 360 to 630°C with values in the 0.09–0.16  $\Omega \cdot \text{mm}$  range for as-alloyed samples. The measured contact resistance drops to the 0.02–0.07  $\Omega \cdot \text{mm}$  range after Ti/Au overlayer evaporation. This five-fold reduction in  $R_c$  shows that the alloyed ohmic pad has a significant resistance and confirms that high conductivity overlayers are required in device applications.

A number of samples with different Si implant parameters and/or implant annealing temperatures were processed under identical conditions. An alloying temperature of 400°C was selected and the Ti/Au interconnect layer was deposited on all of them. Figure 2 shows the resulting measurements of contact

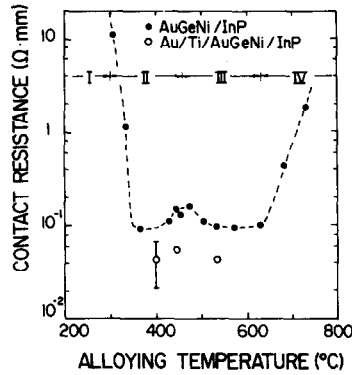


Fig. 1. Measured contact resistance per unit length (specific transfer resistance) vs alloying temperature. ●: Indicate as-alloyed samples. ○: Measurements after further deposition of a Ti/Au interconnect layer over the alloyed ohmic pads. Note the four regimes of interaction of the AuGeNi/InP metallization system indicated on the top of the figure.

resistance vs  $n$ -layer sheet resistance,  $R_{sh}$ , for a large number of TLM's. The two broken lines include all TLM fits which gave regression coefficients better than 0.9999 (all points outside the broken lines have regression coefficients lower than this value). Notice that a very strong correlation (close to quadratic) exists between  $R_c$  and  $R_{sh}$ .

For the standard Si implant (dose:  $5 \times 10^{13} \text{ cm}^{-2}$ , energy 100 keV) and annealing (750°C, 4 s) conditions, the  $R_c$  distribution has a mean value of  $0.044 \Omega \cdot \text{mm}$  and a standard deviation of  $0.023 \Omega \cdot \text{mm}$ . Lower values of  $R_c$  are to be expected by optimizing the implant and annealing parameters. If the semiconductor sheet resistance underneath the metal is taken to be equal to that of the implanted region between ohmic pads, as commonly assumed in the literature, a minimum specific contact resistance of  $6.5 \times 10^{-8} \Omega \cdot \text{cm}^2$  can be deduced. This assumption, however, cannot be assessed with the present TLM structure[6].

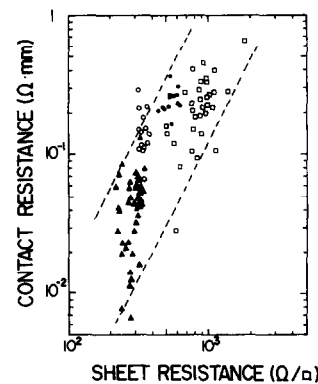


Fig. 2. Contact resistance vs sheet resistance of the underlying  $n$ -InP layer for a number of samples with different Si implantation and annealing conditions (▲  $5 \times 10^{13} \text{ cm}^{-2}$ , 100 keV, 750°C; ●, □  $5 \times 10^{13} \text{ cm}^{-2}$ , 100 keV, 700°C; ○  $5 \times 10^{13} \text{ cm}^{-2}$ , 50 keV 650°C). Ohmic pads are covered by a Ti/Au interconnect layer.

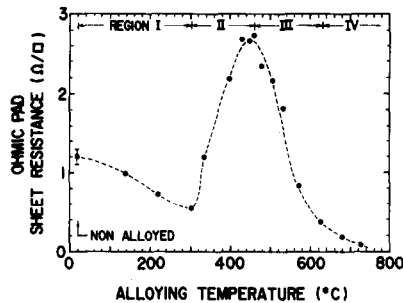


Fig. 3. Ohmic pad sheet resistance of alloyed AuGeNi/InP vs alloying temperature. At the top of the figure, the four regimes of interaction of the AuGeNi/InP system are indicated.

The ohmic pad sheet resistance (alloyed metal-semiconductor layer structure) versus alloying temperature is displayed in Fig. 3. The most prominent feature of this result is a large peak in the value of  $R_m$  at about 450–470°C. Note that this peak coincides with a smaller peak in  $R_c$ , as shown in Fig. 1. This correlation confirms that the metal resistance cannot be completely separated from the contact resistance in the TLM structure if the former is significant[11].

The surface roughness is plotted in Fig. 4 as a function of alloying temperature. Below 460°C the roughness of the ohmic pad is about 100 Å, independently of the alloying temperature. This value is probably limited by the resolution of the measuring instrument. Over 460°C, the roughness increases rapidly. At a temperature of 730°C, the value, off scale in Fig. 4, is 1.27  $\mu$ m.

The edge definition, as observed by scanning electron microscopy, was better than 0.1  $\mu$ m at all alloying temperatures below 730°C. At 730°C, about 2  $\mu$ m contact spreading was observed. The extensive spreading observed by Keramidas *et al.*[12] in Au contacts to InP at temperatures higher than 400°C does not occur in our work, probably due to the shorter alloying time of our experiment (over 3 min in Ref. [12]).

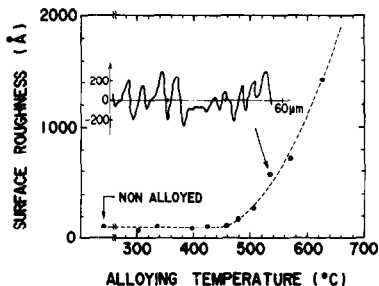


Fig. 4. Surface roughness of the ohmic pads vs alloying temperature. The inset shows a typical measurement on the surface of an ohmic pad. Surface roughness is defined as the maximum peak to valley difference observed in a 60  $\mu$ m length scan over the surface of the contact.

## DISCUSSION

Four different regimes are observed in the alloying temperature behavior of the AuGeNi/InP system (see top of Figs 1 and 3). In the following lines, these four regimes are discussed.

### (a) Region I ( $T \leq 300^\circ\text{C}$ )

In this regime, the contacts are non-ohmic, the surface morphology is very smooth without any features being noticeable by optical or scanning electron microscopy, and the ohmic pad sheet resistance decreases with temperature (Fig. 3). Auger sputtering profiling [Figs 5(a) and 5(b)] showed that, upon annealing at 220°C, Ge migrated out of the AuGe layer into the Ni top layer. This occurrence appears to be independent of the substrate upon which the AuGeNi system is deposited, or the relative

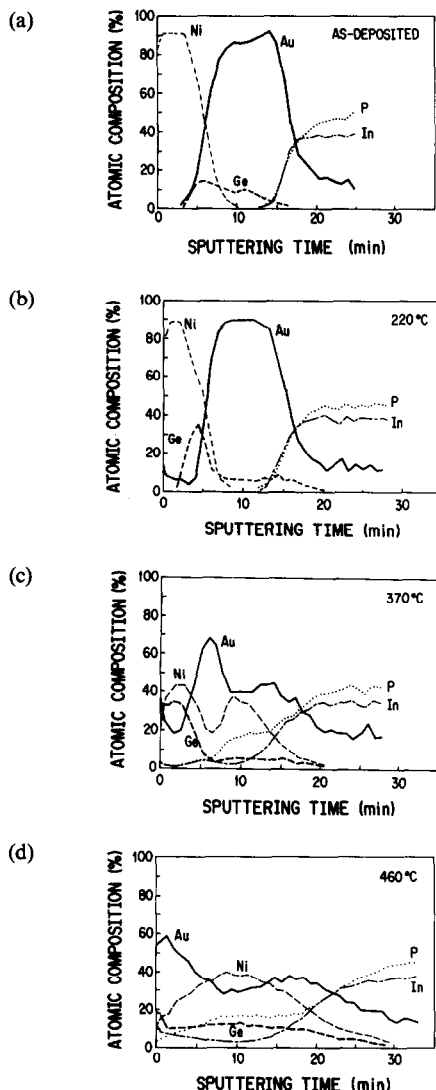


Fig. 5. Sputter Auger profiles of samples alloyed at selected temperatures: (a) as-deposited, (b) 220°C, (c) 370°C, (d) 460°C.

order of deposition of these elements, as Wittmer *et al.* found on an inert  $\text{SiO}_2$  substrate[13]. The ohmic pad resistivity therefore decreases as Ge diffuses out of the AuGe film, rendering it Au rich.

(b) *Region II* ( $300^\circ\text{C} \leq T \leq 460^\circ\text{C}$ )

The contacts become ohmic at about  $300^\circ\text{C}$ . This observation agrees with other authors that have studied the AuGeNi/InP system[14,15]. Studies of the Au/InP system indicate that ohmic contact formation does not occur until about  $400^\circ\text{C}$ [14,16,17] for short alloying times. On the contrary, the Ni/InP system becomes ohmic at  $300^\circ\text{C}$ [14] and the AuGe/InP system at about  $320^\circ\text{C}$ [17]. It is then unclear which mechanism is responsible for ohmic contact formation in the AuGeNi/InP system. In agreement with previous observations of Erickson *et al.*[14], the Auger profile of our sample alloyed at  $370^\circ\text{C}$  (Fig. 5c) showed prominent migration of Ni from the top surface to the InP interface. Graham *et al.*[18], in fact, observed  $\text{Ni}_2\text{P}$  and  $\text{NiP}_2$  in a AuGeNi/InP metallization alloyed at temperatures between 300 and  $400^\circ\text{C}$ . These compounds could be responsible for ohmic contact formation since Appelbaum *et al.*[19] have recently achieved non-alloyed ohmic contacts on *n*-InP using sputtered  $\text{Ni}_2\text{P}$ . On the other hand, Sands *et al.*[20] have found a crystalline  $\text{Ni}_x\text{InP}$  phase after annealing a Ni/InP bilayer at  $300^\circ\text{C}$ . In addition to Ni, AuGe or more complex phases of the involved elements may be responsible for the observed ohmic contact formation at around  $300^\circ\text{C}$  in the AuGeNi/InP system.

The increase of  $R_m$  that occurs in this regime, however, is probably associated with the consumption of Au in its reaction with the InP substrate to form various Au-In alloys and  $\text{Au}_2\text{P}_3$ . The formation of  $\alpha$ -Au,  $\text{Au}_4\text{In}$ ,  $\text{Au}_3\text{In}$  and  $\text{Au}_7\text{In}_2$  has been observed in the Au/InP system for alloying temperatures between  $300^\circ\text{C}$  and  $340^\circ\text{C}$ [17,21-23].  $\text{Au}_2\text{P}_3$  is also reported to form at temperatures around  $320^\circ\text{C}$  in the same metallization system[17,21,23]. In this regime the reactions between Au and In, and Au and P occur in the solid state, preserving the smooth surface morphology of the contact (Fig. 4).

(c) *Region III* ( $460^\circ\text{C} \leq T \leq 630^\circ\text{C}$ )

At about  $460^\circ\text{C}$ ,  $R_m$  reaches a maximum and starts to decrease. This is accompanied by the onset of roughness of the ohmic pad surface, which increases rapidly with temperature (Fig. 4). Decomposition of the InP substrate is observed in the auger profile of the sample alloyed at  $460^\circ\text{C}$  with a considerable spread of Au, Ni and Ge (Fig. 5d). This temperature approximately coincides with the lowest eutectic melting point of the Au-In binary system at  $451^\circ\text{C}$ [24]. A Au-In liquid phase therefore occurs during alloying that results in degradation of the contact morphology upon cooling and enhanced intermixing of the involved elements.

A further consequence of the appearance of a liquid phase is the sudden evaporation of P, as observed in the Au/InP system at  $440^\circ\text{C}$ [25,26]. P appears to evaporate from the InP substrate[23] which, as a result, releases free In (observed in our Auger profiles of Fig. 5(d) and in those of Ref. [16]). This free In may be responsible for the reduction of  $R_m$  observed in this regime. At higher alloying temperatures, more In becomes available (see Auger profile at  $520^\circ\text{C}$ , Fig. 6a), further intermixing occurs promoted by the presence of an extended liquid phase, and large roughening of the contact results upon cooling.

(d) *Region IV* ( $T \geq 630^\circ\text{C}$ )

Beyond  $630^\circ\text{C}$  the contact resistance starts to degrade due to extensive decomposition of the InP. Free In becomes available in ever larger quantities which further reduces the pad sheet resistance. The Auger profile of a sample alloyed at  $730^\circ\text{C}$  revealed the presence of a high In concentration at the top surface (Fig. 6b). It appears that the InP substrate has melted to a large depth producing a very rough surface. The liquid phase poured out of the edges of the ohmic pads at this temperature resulting in a poorly defined edge.

## CONCLUSIONS

From the examination of contact resistance, surface morphology, and edge definition, a practical alloying temperature window of application of AuGeNi ohmic contacts to *n*-InP for FETs spans from about 360 to  $630^\circ\text{C}$ . Since a liquid phase appears at an alloying temperature of about  $460^\circ\text{C}$ , good contacts with a perfectly smooth surface morphology can be obtained from 360 to  $460^\circ\text{C}$ . An average value of  $0.044 \Omega \cdot \text{mm}$  of specific transfer

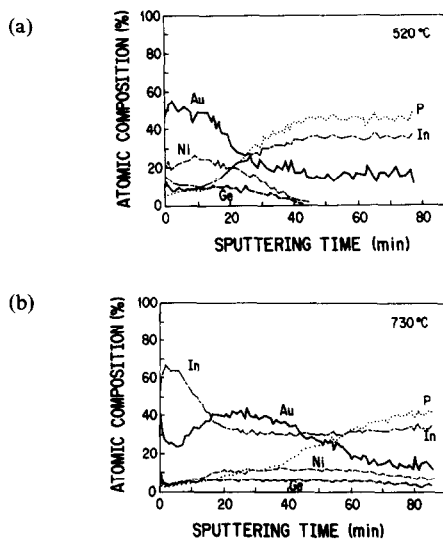


Fig. 6. Sputter Auger profiles of samples annealed at selected temperatures: (a)  $520^\circ\text{C}$ , (b)  $730^\circ\text{C}$ .

resistance has been obtained at 400°C. Lower values are expected by reducing the sheet resistance of the underlying *n*-InP.

## REFERENCES

1. T. Itoh and K. Ohata, *IEEE Trans. Electron Dev.* **ED-30**, 811 (1983).
2. J. del Alamo and T. Mizutani, *IEEE Electron Dev. Lett.* **EDL-8**, 220 (1987).
3. T. H. Windhorn, L. W. Cook, M. A. Haase and G. E. Stillman, *Appl. Phys. Lett.* **42**, 725 (1983).
4. S. M. Sze, *Physics of Semiconductor Devices*, p. 47. Wiley, New York (1981).
5. B. Tell, A. S. H. Liao, K. F. Brown-Goebeler, T. J. Bridges, G. Burkhardt, T. Y. Chang and N. S. Bergano, *IEEE Trans. Electron Dev.* **ED-32**, 2319 (1985).
6. E. Yamaguchi, T. Nishioka and Y. Ohmachi, *Solid-St. Electron.* **24**, 263 (1981).
7. Y. Nishitani and T. Kotani, *J. Electrochem. Soc.* **126**, 2269 (1979).
8. J. del Alamo and T. Mizutani, *J. appl. Phys.* **62**, 3456 (1987).
9. G. K. Reeves and H. B. Harrison, *IEEE Electron Dev. Lett.* **EDL-3**, 111 (1982).
10. F. Lonnrum and J. S. Johannessen, *Electron. Lett.* **22**, 632 (1986).
11. B. Kovacs and I. Mojzes, *IEEE Trans. Electron Dev.* **ED-33**, 1401 (1986).
12. V. G. Keramidas, H. Temkin and S. Mahajan, *Inst. Phys. Conf. Ser.* Vol. 56, p. 293 (1980).
13. M. Wittmer, R. Pretorius, J. W. Mayer and M.-A. Nicolet, *Solid-St. Electron.* **20**, 433 (1977).
14. L. P. Erickson, A. Waseem and G. Y. Robinson, *Thin Solid Films* **64**, 421 (1979).
15. E. Kuphal, *Solid-St. Electron.* **24**, 69 (1981).
16. H. B. Kim, A. F. Lovas, G. G. Sweeney and T. M. S. Heng, *Inst. Phys. Conf. Ser.* Vol. 33b, p. 145 (1977).
17. P. Auvray, A. Guivarc'h, H. L'Haridon, J. P. Mercier and P. Henoc, *Thin Solid Films* **127**, 39 (1985).
18. R. J. Graham and J. W. Steeds, *Inst. Phys. Conf. Ser.* Vol. 67, p. 507 (1983).
19. A. Applebaum, M. Robbins and F. Schrey, *IEEE Trans. Electron Dev.* **ED-34**, 1026 (1987).
20. T. Sands, C. C. Chang, A. S. Kaplan, V. G. Keramidas, K. M. Krishnan and J. Washburn, *Appl. Phys. Lett.* **50**, 1346 (1987).
21. A. Piotrowska, P. Auvray, A. Guivarc'h, G. Pelous and P. Henoc, *J. appl. Phys.* **52**, 5112 (1981).
22. J. M. Vandenberg, H. Temkin, R. A. Hamm and M. A. DiGiuseppe, *J. appl. Phys.* **53**, 7385 (1982).
23. C. T. Tsai and R. S. Williams, *J. Mater Res.* **1**, 820 (1986).
24. M. Hansen, *Constitution of Binary Alloys*, p. 210. McGraw-Hill, New York (1958).
25. I. Mojzes, D. Szigethy and R. Veresegyhazy, *Electron. Lett.* **19**, 117 (1983).
26. I. Mojzes, R. Veresegyhazy and V. Malina, *Thin Solid Films* **144**, 29 (1986).